Hindawi
Advances in Materials Science and Engineering
Volume 2020, Article ID 8024803, 9 pages
https://doi.org/10.1155/2020/8024803

Research Article

Comparison of Bending Fatigue of NiTi and CuAlMn Shape Memory Alloy Bars

Haoyu Huang,[1] **Yuan-Zhi Zhu**,[2] **and Wen-Shao Chang**[3]

[1]*Beijing Key Lab of Earthquake Engineering and Structural Retrofit, The Key Laboratory of Urban Security and Disaster Engineering of Ministry of Education, Beijing University of Technology, Beijing 100124, China*
[2]*School of Mechanical and Materials Engineering, North China University of Technology, Beijing 100144, China*
[3]*School of Architecture, University of Sheffield, Sheffield S10 2TN, UK*

Correspondence should be addressed to Wen-Shao Chang; w.chang@sheffield.ac.uk

Received 21 October 2019; Accepted 25 November 2019; Published 14 January 2020

Academic Editor: Davide Palumbo

The behaviour under cyclic bending and in particular the fatigue properties of shape memory alloy (SMA) bars are important for civil engineering applications. In this paper, structural and functional fatigue is studied for both NiTi- and copper-based shape memory alloys. The results are presented from cyclic bending tests on 7 mm diameter NiTi and 12 mm diameter CuAlMn SMA bars targeted at 100,000 cycles. During the tests, dynamic loading at 1 Hz, 5 Hz, and 8 Hz was applied for different strain levels (0.5%, 1%, 2%, and 6%). The stress-strain curve, damping ratio, and secant stiffness were analysed for material characterisation, and the evolution of these parameters was studied to assess functional fatigue. The fatigue life is extended dramatically when the strain is below 1%, and the structural fatigue life of CuAlMn is shown to be better than that of NiTi and to depend on the loading rate. However, decay in stiffness can be found in the CuAlMn SMA, which is considered to be caused particularly by its long grain boundary.

1. Introduction

Shape memory alloy (SMA) has been developed in different fields of civil engineering as indicated by previous review papers [1–3]. Cyclic loading is a common feature of applications. For example, SMAs have been studied as an energy dissipater in seismic devices [4–6], which work in repeated motions. Despite big deformations, SMA installed in civil structures is also expected to withstand a large number of minor oscillations due to the actions of wind [7]. Considering using SMA in active control systems such as tuned mass damper or tuned vibration absorber [8–10], superior and stable cyclic and fatigue behaviours are required in long-term vibration reduction. Therefore, the fatigue behaviour of SMA is an important area of study regarding both big deformations and small deformations, and it is also of importance to study the material characteristics during cyclic loading life.

The fatigue behaviours of SMA can be divided into structural fatigue and functional fatigue [11, 12]. Structural fatigue indicates the property decaying caused by accumulation of microstructural damages such as cracks until failure. Functional fatigue is a degradation of the shape memory effect or damping capacity of superelastic SMA due to plasticity. Fatigue life defined in this study is the number of cycles to failure under a given amplitude of strain. Tobushi et al. [13] and Miyazaki et al. [14] created bending-rotating fatigue (BRF) testing methods for wires. The BRF method means a SMA wire is bent by displacement control to form a half cycle for a number of cycles. Sawaguchi et al. [15] and Miyazaki et al. [14] tested NiTi wires under different loading rates, applying BRF methods. When strain was no less than 1%, the rupture cycles strongly depended on the strain, whilst the fracture cycles became insensitive to the strain when lesser than 1%. Tensile cyclic testing is a general and popularly used fatigue testing method. Miyazaki et al. [16] and Moumni et al. [17] did the fatigue analysis on NiTi-based SMA by cyclic tension. The results present the same trend and strongly suggest that fatigue life reduces with stress levels. By these two loading methods, the fatigue life all

grows dramatically under a small strain level and the length of fatigue life present slight differences at the same strain. More fatigue resistance properties of NiTi SMA are reviewed by Robertson et al. [18]. However, it can be seen that all of the bending tests on SMA in previous research were conducted on wires.

The fatigue life depends on the loading conditions, specimens, and material preparation. To achieve long fatigue life for SMA, the effect factors such as working temperature, sample dimensions, loading rate, grain size, and metal surface condition are of concerns. The lower temperature SMA has the longer fatigue life it can sustain with the same strain level [14, 19]. The reason can be explained by previous research about the temperature effect [20], and the critical transformation stress increases at a higher temperature based on the Clausius–Clapeyron relationship. Regarding the influence of the loading rate, Sawaguchi et al. [15] tested NiTi-based SMAs and showed that when the maximum strain was greater than 1%, the dependence of fatigue life on the loading rate was strong, meaning that a lower loading rate can lead to a longer fatigue life. Nevertheless, this dependence became weak when decreasing the strain level below 1% strain. Further studies should highlight the loading rate effect on the fatigue of copper-based SMAs as this behaviour on copper-based SMA is rarely studied. The grain size can strongly influence fatigue properties. According to Siredey et al. [21], single-crystal CuAlBe supports a much longer fatigue life than CuAlBe polycrystal SMAs, especially for strains bigger than 4%. For CuAlNi SMAs, Van Humbeeck [22] demonstrated that cracks always occur near or at grain boundaries for polycrystals because grain boundaries show brittle features [23]. There are other effects which can affect the fatigue life such as material treatment, material composition (e.g., NiTi- and copper-based SMA), and material phase (e.g., austenite and martensite).

Fatigue life is a classical approach presenting the number of cycles to fracture to assess the structural fatigue, which can be applied to most of the metal materials. However, functional fatigue is a particular behaviour shown in cyclic loading on SMA, which is found by the gradual decreasing damping ratio and increasing plasticity during the cyclic superelastic deformations [11,24–29]. To find out the reason of inducing functional fatigue, it is worthwhile noting that, in the first few cycles, critical stress for phase transformation decreases and then becomes stable. This is found to be because of dislocation slip during stress-induced transformation [30]. Casati et al. [31] indicated new dislocation substructures are formed in these cycles, which causes a larger residual strain and the loss of shape memory. The internal stress contributed by the dislocation can facilitate the formation of martensite, so it is the reason why the transformation stress drops in the next cycles [25]. As a result, it causes the decrease in dissipated energy. To obtain stable superelastic behaviour during service, "pretraining" procedures including cyclic training, thermomechanical training, and cold work/annealing before the application are required.

Concerning the aforementioned previous research results which have studied the effects on the fatigue of both copper-based SMAs and NiTi SMAs, however, the fatigue behaviours vary depending upon different testing conditions and should be studied with specific regard to strain levels and specimens, especially needing studies for copper-based SMA and SMA bars with respect to civil structural applications. Unlike SMA wires under bending, bending of bars has a dissymmetry effect, which means the neutral plane can move during cyclic loading; in this case, fatigue behaviours of SMA bars under bending need to be particularly studied [32].

In aspect of engineering application, SMA bar bending is suggested to be of importance in civil structures [33, 34]. They studied SMA bar bending employed in bridges in order to enhance seismic performance and indicated bending is more appropriate because in tensile SMA applications especially during earthquakes, SMA bars can be easily in compression which leads to buckling issues.

Concerning the importance in civil structures, what this paper will discuss are fatigue life and functional fatigue of SMA bars under bending, whereby demonstrating the fatigue behaviours and the cause of formation. In civil engineering practice, SMAs sustain both low-strain deformations, e.g., under wind and human-induced vibration, and high-strain deformations, e.g., under earthquake. In the design stage of using SMAs, it is significant to know the damping behaviours and fatigue performance of SMAs both in low and high strain levels even though there is little or no phase transformation at the low strain level. Also, different types of SMAs could perform differently in low and high strain levels; in this study, both NiTi and CuAlMn SMA bars were employed; therefore, a 3-point bending testing rig was designed at first. Different dynamic loading frequencies and deformation procedures were performed so as to study the frequency effect and fatigue life. The stress-strain curve, damping ratio, secant stiffness, and fatigue life of the bars were analysed.

2. Materials and Methods

In this study, superelastic NiTi bars (diameter 7 mm and length 125 mm) and superelastic CuAlMn bars (diameter 12 mm and length 125 mm) are provided by Nitinol Devices and Components, Inc., USA, and Furukawa Techno Material Co., Ltd., Japan, respectively. The chemical composites of NiTi and CuAlMn SMA are Ni = 52.2 wt.% and Ti = 47.8 wt.% and Cu = 81.9 wt.%, Al = 7.4 wt.%, and Mn = 10.7 wt.%, respectively. According to the material providers, the transformation temperature A_f of NiTi is −40°C while that of CuAlMn is −39°C. Both NiTi and CuAlMn samples were polished and have the similar surface conditions. It is worthwhile noting that CuAlMn SMA in this study has a big grain size even more than the diameter, and it can be seen there are clear boundaries along the longitudinal direction (Figure 1). This has been described as a "bamboo-like" structure by Sutou et al. [35].

To conduct bending tests on alloy bars, a 3-point bending rig, as shown in Figure 2, was manufactured. The specimen bar (point 4) was supported by two rounded bearings (points 1 and 2). The space between the two

Figure 1: CuAlMn SMA bar with a bamboo-like grain structure.

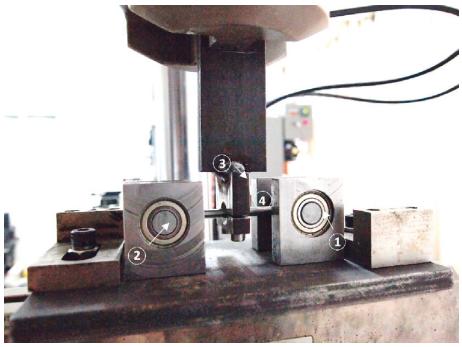

Figure 2: Bending testing rig.

bearings was 100 mm. At the middle of the specimen bar, a steel plate (point 3) can pull and push the specimen to a specified displacement.

The cyclic bending tests were performed at room temperature around 25°C, with an air conditioner beside the rig which can maintain the constant ambient temperature. Four strain levels were selected, 0.5%, 1%, 2%, and 6%, and there were three loading frequencies, 1 Hz, 5 Hz, and 8 Hz, performed for a small strain level, as shown in Table 1. Then, the SMA bars completed each loading procedure using a triangle waveform under displacement control for 100,000 cycles at most. During these tests, time, displacements, and forces were recorded by data logger.

The maximum displacement for small strain levels (0.5% and 1%) set on the machine was calculated using the following equations:

$$\varepsilon = \frac{d}{2R}, \qquad \varepsilon = \frac{d \times x}{x^2 + a^2}, \tag{1}$$

where x = the displacement of the machine, d = diameter of specimen, R = radius of curvature, and a = half of the free length of specimen.

Concerning that the deformation becomes not linear at bigger strain levers (2% and 6%), the strain is calculated by

$$\varepsilon = \frac{(\theta/360) \times \pi(2R + d) - 2a}{2a}, \tag{2}$$

where θ is the bending angle of the sample. It is notable that ε represents the strain only in tension side.

3. Results

Figures 3 and 4 show the stress-strain graphs of NiTi and CuAlMn SMAs, and the stress presenting here is the maximum stress at the largest bending moment position. According to the curve, it can be clearly seen that NiTi SMA specimens do not transform to the martensitic phase from austenite at 0.5% and 1% strain. For the NiTi 2% strain level, there is a partial transformation due to superelasticity. However, the CuAlMn SMA starts partial transformation at 1% strain, which indicates that the transformation strain of the CuAlMn is smaller than that of the NiTi SMA.

Table 1: Parameters of cyclic loading.

Strain	0.5%	1%	2%	6%
Frequency	1 Hz 5 Hz 8 Hz	1 Hz 5 Hz 8 Hz	1 Hz	1 Hz

Compared with the NiTi stress-strain graphs, the CuAlMn SMAs show obvious structural fatigue since the stiffness decays gradually. This structure fatigue usually started early than that from half of its fatigue life. From observation of the specimen surface during testing, crack frequently appears on CuAlMn specimens, which leads to stiffness decaying (Figure 4). For example, Figure 5 shows the crack on the CuAlMn sample surface in the condition of 0.5% at 5 Hz. Gradual accumulation of microstructural damage can cause property decaying and the fracture of material [11].

Considering the damping behaviours of SMAs, Figures 6 and 7 present the damping ratio evolution at 1 Hz, 5 Hz, and 8 Hz for 0.5% and 1% strain. The damping ratio is calculated by

$$\xi = \frac{\Delta\omega}{4\pi\omega}, \tag{3}$$

where $\Delta\omega$ is the dissipated energy and ω is the equivalent elastic strain energy. The detailed approaches calculating the damping ratio in this study are referred from the book by Priestley and Seible [36].

Some of the evolutions of the damping ratio with cycles show functional fatigue (Figures 6 and 7). Damping ratio drops dramatically during the first cycle and then decreases gently and keeps stable in the following cycles such as the evolution in 8 Hz 1% NiTi and 5 Hz and 8 Hz 0.5% CuAlMn. The reason for the functional fatigue was revealed by previous research, and it may be due to the internal stress contributed by dislocation slip aforementioned. As seen in 8 Hz 1% CuAlMn, there is a scatter due to the deficient sampling rate during measurement at such a high loading rate but does not affect the studies for cyclic behaviours.

Figure 8 shows the averaged damping ratio after 100 cycles for 0.5%, 1%, and 2% strain and averaged damping ratio after 10 cycles for 6% strain; a higher strain level leads to a higher damping ratio, and the frequency dependence

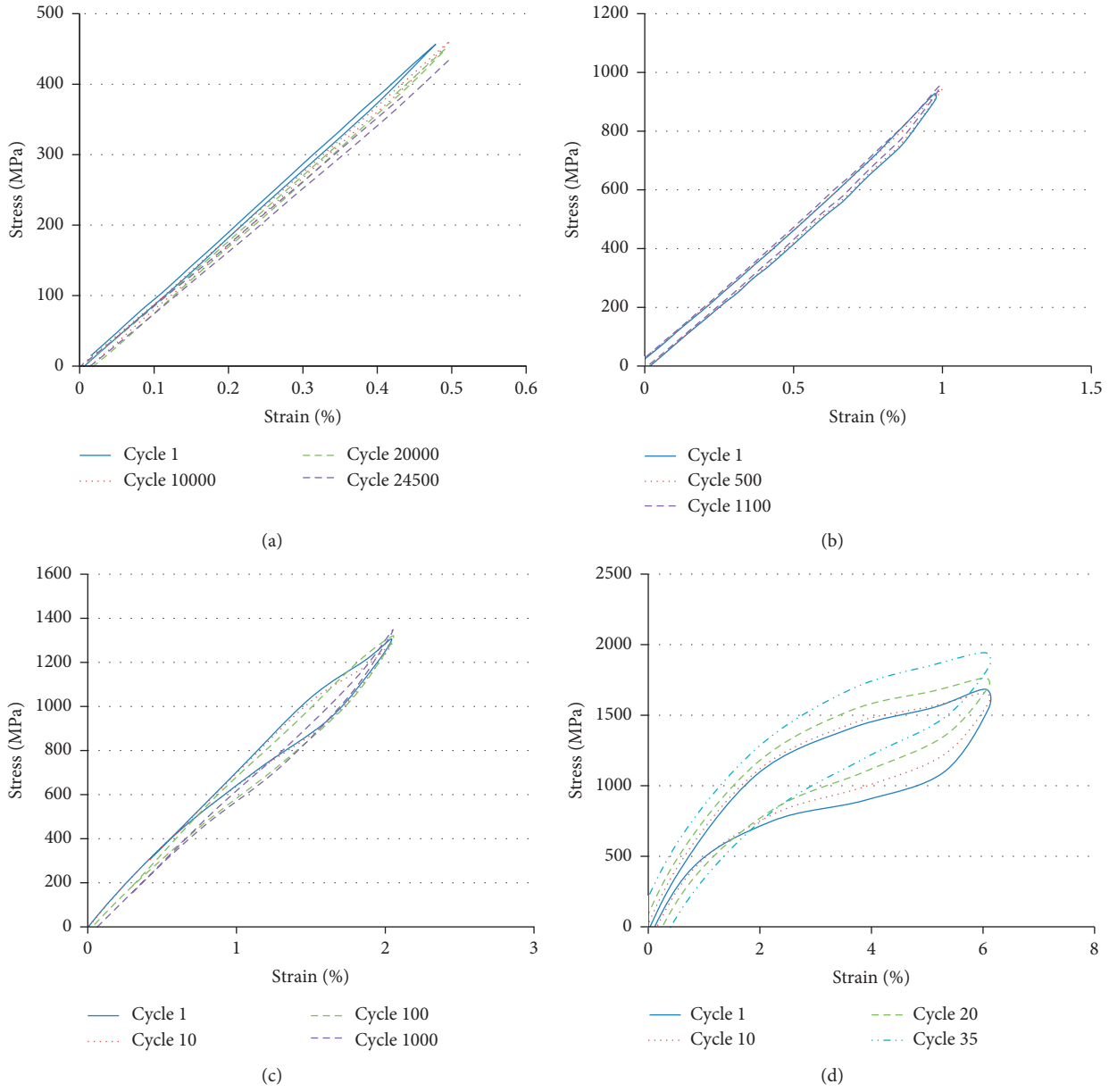

Figure 3: Cyclic loading stress-strain graphs at 1 Hz of NiTi SMAs: (a) 0.5%; (b) 1%; (c) 2%; (d) 6%.

can be clearly seen. In comparison, CuAlMn SMAs have a better damping capacity than NiTi SMAs. The transformation starting stress of NiTi SMA is high, and it is in elastic deformation or partial transformation from 0.5% to 2% strain levels; the damping ratio of NiTi therefore is low at this range.

Considering the superelastic properties of SMAs, secant stiffness is appropriate to reflect the stiffness of specimens. The equation for secant stiffness is defined as follows:

$$K = \frac{\sigma_{\max} - \sigma_{\min}}{\varepsilon_{\max} - \varepsilon_{\min}}, \quad (4)$$

where $\sigma_{\max}$, $\sigma_{\min}$ and $\varepsilon_{\max}$, $\varepsilon_{\min}$ represent the maximum and minimum stress and strain in each hysteresis, respectively. The stress ($\sigma_{\max}$ and $\sigma_{\min}$) is taken from the value at the maximum bending moment position.

Figure 9 compares the averaged secant stiffness for NiTi SMAs after 100 cycles in each loading condition. Figure 10 shows the averaged secant stiffness at the stabilised plateau (stabilised cycles) for CuAlMn SMAs. In terms of NiTi, it can be seen that the stiffness is insensitive to dynamic frequencies from 1 Hz to 8 Hz. Secant stiffness at 0.5% strain decreases about 4 GPa with an increasing loading rate. There are bigger differences for CuAlMn SMAs between 1 Hz, 5 Hz, and 8 Hz, and there is a decline at 0.5% strain, while the secant stiffness rises at the 1% strain level with the increasing loading rate. To put into contrast, it is notable that when the frequency is above 5 Hz, the stiffness of NiTi changes slighter than that of CuAlMn. From Figures 9 and 10, the stiffness of CuAlMn SMAs is less than that of NiTi.

Figure 11 shows the fatigue life of NiTi SMAs and CuAlMn SMAs. CuAlMn SMAs are highly dependent on

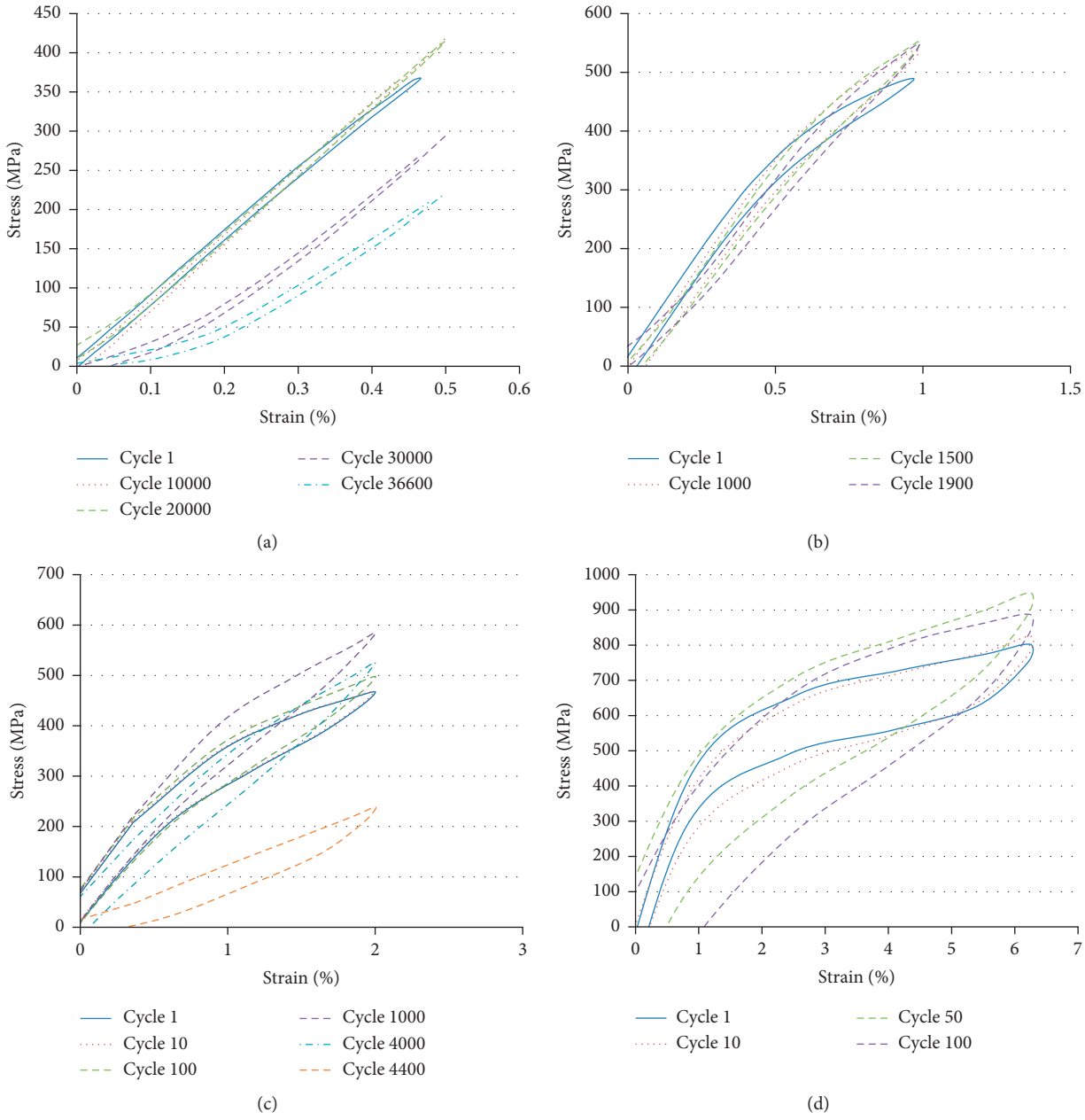

Figure 4: Cyclic loading stress-strain graphs at 1 Hz of CuAlMn SMAs: (a) 0.5%; (b) 1%; (c) 2%; (d) 6%.

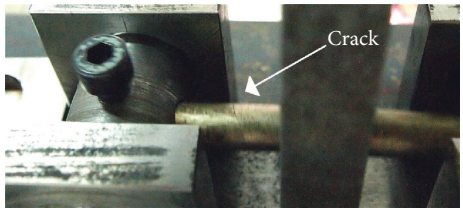

Figure 5: Crack appears on the CuAlMn specimen surface during test.

frequency, and the strain-fatigue life graph illustrates that the fatigue life is longer when the frequency is higher. To be clear, the CuAlMn specimen did not fracture after 100,000 cycles for 0.5% strain at 8 Hz, which shows superior fatigue property in this condition. By contrast, the fatigue life of the NiTi SMA is less dependent on the frequency. In comparison, CuAlMn SMAs show a better structural fatigue life than NiTi under cyclic bending. There is an obvious turning trend in fatigue life of NiTi and CuAlMn SMAs. When the strain level is below 1%, the fatigue life can be increased dramatically.

To anticipate the fracture position of specimens, it may be located in the position of the maximum bending moment, which is in the middle of the specimen. All of the NiTi bars broke in the middle, while most of CuAlMn bars fractured at the grain boundary rather than the point of maximum bending moment. It can be seen that the grain boundary is a weak area in which it is easy to induce cracks.

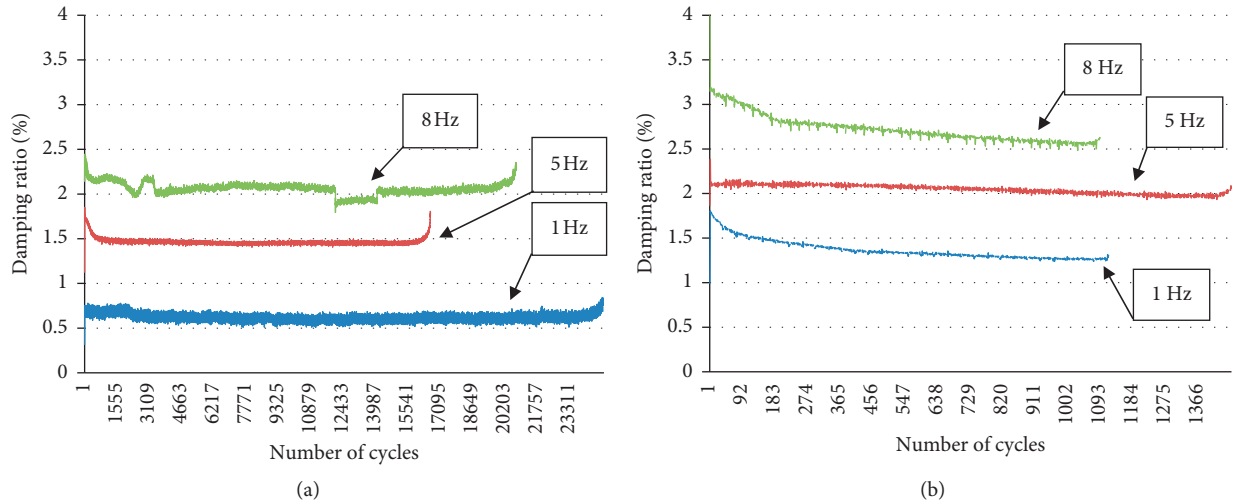

Figure 6: Evolution of the damping ratio at 1 Hz, 5 Hz, and 8 Hz of NiTi SMAs: (a) 0.5% strain; (b) 1% strain.

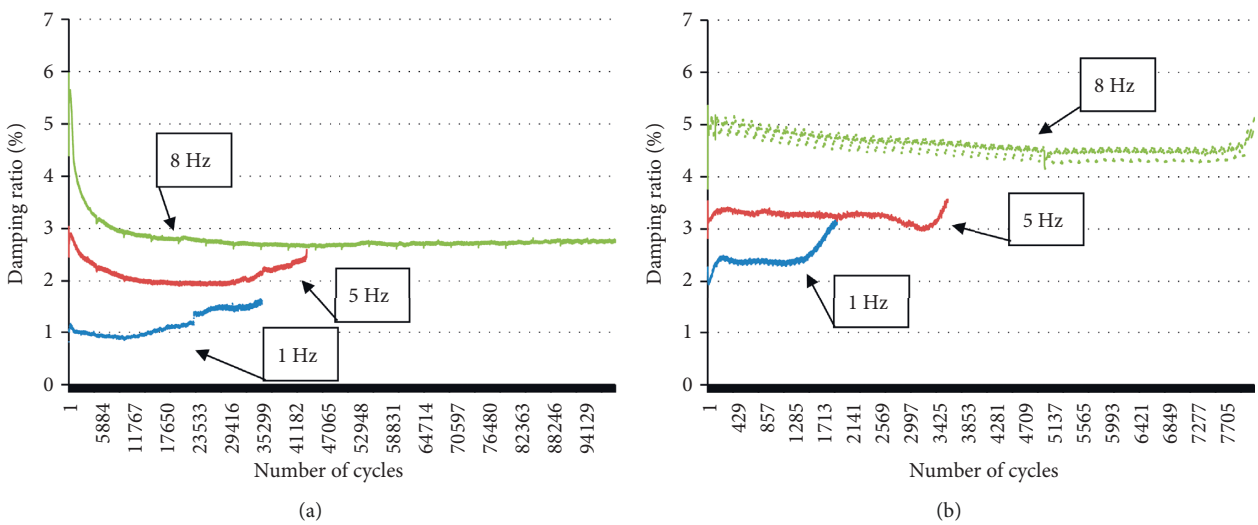

Figure 7: Evolution of the damping ratio at 1 Hz, 5 Hz, and 8 Hz of CuAlMn SMAs: (a) 0.5% strain; (b) 1% strain.

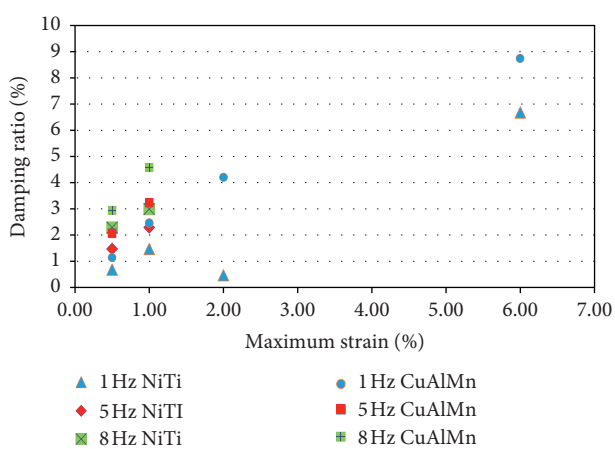

Figure 8: Comparison of the damping ratio on average.

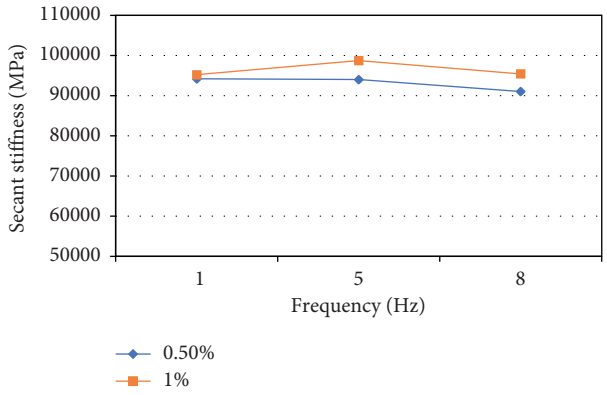

Figure 9: Comparison of the stiffness of each loading procedure on NiTi SMAs.

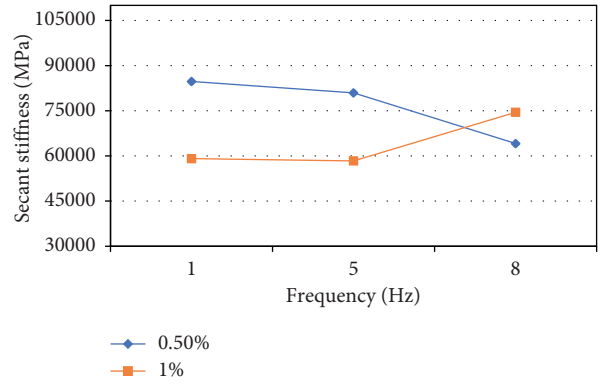

Figure 10: Comparison of the stiffness of each loading procedure on CuAlMn SMAs.

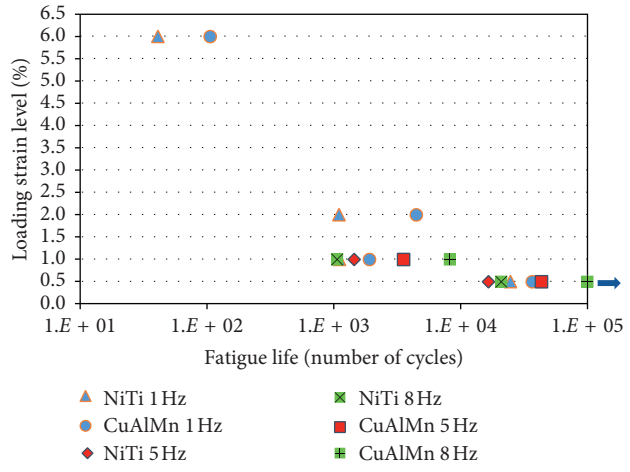

Figure 11: Fatigue life of NiTi and CuAlMn SMAs.

4. Discussion

As aforementioned, the effect of the loading rate is associated with the SMA thermomechanical property, as can be illustrated as the Clausius–Clapeyron coefficient, which presents the relationship between working temperature and stress. The effect of the loading rate therefore does not react at the relatively constant temperature. For example, Leo et al. [37] tested NiTi SMA wires at different loading rates (0.5, 5, and 50 mm/min). They controlled the specimens' temperature constant using surrounding media, and the results showed that the effect of the loading rate became insensitive. Bearing this in mind, as regarding this study focused on fatigue, loading rate dependence for NiTi SMA is weak. The reason is when the strain level is small, the phase transformation from austenite to martensite does not occur; the dissipated energy therefore is relatively low, and hence, specimen keeps a constant temperature.

This paper presents a new finding that the fatigue life of CuAlMn SMA increases with the loading frequencies as there is no study worked on the frequency effect on fatigue life of copper-based SMA. The only comparison can be done is taken concern of Casciati and Marzi [19]'s work at 0.5 Hz loading and Torra et al. [7]'s work at 1 Hz loading, and the fatigue life of CuAlBe SMA at 1 Hz is more than that at 0.5 Hz for about 6000 cycles under small stress levels (200 MPa–300 MPa).

With respect to the earlier structural fatigue behaviours of CuAlMn indicated in this study, the reason might be due to the big grain size, and it is easy to induce the crack at such a long grain boundary. As illustrated by Van Humbeeck [22] and Gloanec [23], grain boundary is a weak area for cracks initiation. Due to big grain size and bamboo-like structure of CuAlMn in this study (Figure 1), it can behave like single-crystal SMA, which helps CuAlMn in this study show better structural fatigue life.

According to the damping ratio evolution in this study, not all of the specimens showed functional fatigue and some specimens present stable cyclic behaviours. It can suggest functional fatigue does not always appear because it depends on the dislocation and microstructural slip. It is important to note proper material treatments such as annealing and cold work can avoid functional fatigue.

5. Conclusion

This study presents cyclic fatigue bending tests on SMA bars at different dynamic loading frequencies. In the study, NiTi SMA bars and CuAlMn SMA bars were tested targeting at 100,000 cycles, and different strain levels were imposed. From strain-stress curves, NiTi shows a higher transformation strain. The stiffness decaying of CuAlMn SMAs is observed in the stress-strain graphs; in contrast, the stress-strain curves of NiTi SMAs are constant with cyclic loading. For CuAlMn SMA bars, the fatigue life depends on loading frequency and is longer at higher frequency. However, the fatigue life of NiTi SMA does not show this dependence. The functional fatigue depends on the microstructure of material and is induced by dislocation slip. CuAlMn presents better structural fatigue life than NiTi SMA; however, more experimental results are needed to support this conclusion.

In summary, both CuAlMn and NiTi SMA bars are appropriate to apply in civil engineering with respect to their high damping capacity and stiffness as well as their particular recentring property. Small deformation (<1% strain) conditions are preferred for both types of SMAs because they

are able to present a long fatigue life. High-frequency loading conditions are preferred for CuAlMn as it can effectively improve the fatigue life. In terms of mechanical properties, CuAlMn SMA has a higher damping, while NiTi SMA shows a higher stiffness in all testing conditions. To use NiTi and CuAlMn SMA bars, the effect of frequency on damping capacity requires consideration. For instance, in dynamic applications in order to dissipate more energy, it is more effective to carry out at the higher loading rate. However, to employ CuAlMn SMA bars, the unstable mechanical behaviours along long-term cycling should be taken into concern; especially, grain boundary may lead to stiffness decaying. Also, the change in loading frequency leads to variable secant stiffness of CuAlMn. In the future research, to stabilise and improve the fatigue behaviours of CuAlMn SMA, the approaches to utilise more single-crystal CuAlMn SMA or enhance its grain boundaries will be a direction.

Data Availability

The data used to support the findings of this study are available from the corresponding author upon request.

Conflicts of Interest

The authors declare that they have no conflicts of interest.

Acknowledgments

The authors would like to thank National Natural Science Foundation of China (51908007), Beijing Municipal Education Commission (KM201910005021), and Basic Research Foundation of Beijing University of Technology and International Copper Association (TEK-1079) for their supports. The authors acknowledge that this paper is based on Haoyu Huang's PhD thesis "A Temperature Controlled Semi-Active Tuned Mass Damper Using Shape Memory Alloy for Vibration Reduction Applications". The authors appreciate Nitinol Devices and Components, Inc. and Furukawa Techno Material Co., Ltd. for their material supply.

References

[1] L. Janke, C. Czaderski, M. Motavalli, and J. Ruth, "Applications of shape memory alloys in civil engineering structures—overview, limits and new ideas," *Materials and Structures*, vol. 38, no. 279, pp. 578–592, 2005.

[2] R. Desroches and B. Smith, "Shape memory alloys in seismic resistant design and retrofit: a critical review of their potential and limitations," *Journal of Earthquake Engineering*, vol. 8, no. 3, pp. 415–429, 2004.

[3] O. E. Ozbulut, S. Hurlebaus, and R. Desroches, "Seismic response control using shape memory alloys: a review," *Journal of Intelligent Material Systems and Structures*, vol. 22, no. 14, pp. 1531–1549, 2011.

[4] V. Birman, "Effect of SMA dampers on nonlinear vibrations of elastic structures," in *Proceedings of the SPIE*, vol. 3038, pp. 268–276, San Diego, CA, USA, June 1997.

[5] H. Qian, H. Li, G. Song, and W. Guo, "Recentering shape memory alloy passive damper for structural vibration control," *Mathematical Problems in Engineering*, vol. 2013, p. 13, 2013.

[6] H. W. Ma and C. D. Cho, "Feasibility study on a superelastic SMA damper with re-centring capability," *Materials Science and Engineering A—Structural Materials Properties Microstructure and Processing*, vol. 473, no. 1-2, pp. 290–296, 2008.

[7] V. Torra, A. Isalgue, C. Auguet et al., "Damping in civil engineering using SMA. The fatigue behavior and stability of CuAlBe and NiTi alloys," *Journal of Materials Engineering and Performance*, vol. 18, no. 5-6, pp. 738–745, 2009.

[8] H. Huang, W.-S. Chang, and K. Mosalam, "Feasibility of shape memory alloy in a tuneable mass damper to reduce excessive in-service vibration," *Structural Control and Health Monitoring*, vol. 24, no. 2, p. e1858, 2017.

[9] C. Liang and C. A. Rogers, "Design of shape memory alloy springs with applications in vibration control," *Journal of Intelligent Material Systems and Structures*, vol. 8, no. 4, pp. 314–322, 1997.

[10] K. Williams, G. Chiu, and R. Bernhard, "Adaptive-passive absorbers using shape-memory alloys," *Journal of Sound and Vibration*, vol. 249, no. 5, pp. 835–848, 2002.

[11] G. Eggeler, E. Hornbogen, A. Yawny, A. Heckmann, and M. Wagner, "Structural and functional fatigue of NiTi shape memory alloys," *Materials Science and Engineering A—Structural Materials Properties Microstructure and Processing*, vol. 378, no. 1-2, pp. 24–33, 2004.

[12] T. Ataalla, M. Leary, and A. Subic, "Functional fatigue of shape memory alloys," *Sustainable Automotive Technologies 2012*, vol. 2012, pp. 39–43, 2012.

[13] H. Tobushi, T. Nakahara, Y. Shimeno, and T. Hashimoto, "Low-cycle fatigue of TiNi shape memory alloy and formulation of fatigue life," *Journal of Engineering Materials and Technology*, vol. 122, no. 2, pp. 186–191, 2000.

[14] S. Miyazaki, K. Mizukoshi, T. Ueki, T. Sakuma, and Y. Liu, "Fatigue life of Ti-50 at.% Ni and Ti-40Ni-10Cu (at.%) shape memory alloy wires," *Materials Science and Engineering A—Structural Materials Properties Microstructure and Processing*, vol. 273–275, pp. 658–663, 1999.

[15] T. A. Sawaguchi, G. Kausträter, A. Yawny, M. Wagner, and G. Eggeler, "Crack initiation and propagation in 50.9 At. pct Ni-Ti pseudoelastic shape-memory wires in bending-rotation fatigue," *Metallurgical and Materials Transactions A*, vol. 34, no. 12, pp. 2847–2860, 2003.

[16] S. Miyazaki, Y. Sugaya, and K. Otsuka, "Effects of various factors on fatigue life of NiTi alloys," in *Proceedings of the MRS-International Meeting on Advanced Materials*, pp. 251–262, Tokyo, Japan, May-June 1989.

[17] Z. Moumni, A. V. Herpen, and P. Riberty, "Fatigue analysis of shape memory alloys: energy approach," *Smart Materials and Structures*, vol. 14, no. 5, pp. S287–S292, 2005.

[18] S. W. Robertson, A. R. Pelton, and R. O. Ritchie, "Mechanical fatigue and fracture of Nitinol," *International Materials Reviews*, vol. 57, no. 1, pp. 1–37, 2012.

[19] S. Casciati and A. Marzi, "Experimental studies on the fatigue life of shape memory alloy bars," *Smart Structures and Systems*, vol. 6, no. 1, pp. 73–85, 2010.

[20] B. Andrawes and R. DesRoches, "Effect of ambient temperature on the hinge opening in bridges with shape memory alloy seismic restrainers," *Engineering Structures*, vol. 29, no. 9, pp. 2294–2301, 2007.

[21] N. Siredey, A. Hautcoeur, and A. Eberhardt, "Lifetime of superelastic Cu-Al-Be single crystal wires under bending

fatigue," *Materials Science and Engineering A—Structural Materials Properties Microstructure and Processing*, vol. 396, no. 1-2, pp. 296–301, 2005.

[22] J. Van Humbeeck, "Cycling effects, fatigue and degradation of shape memory alloys," *Le Journal De Physique IV*, vol. 1, no. C4, pp. 189–197, 1991.

[23] A.-L. Gloanec, P. Cerracchio, B. Reynier, A. Van Herpen, and P. Riberty, "Fatigue crack initiation and propagation of a TiNi shape memory alloy," *Scripta Materialia*, vol. 62, no. 10, pp. 786–789, 2010.

[24] H. Soul, A. Isalgue, A. Yawny, V. Torra, and F. C. Lovey, "Pseudoelastic fatigue of NiTi wires: frequency and size effects on damping capacity," *Smart Materials & Structures*, vol. 19, no. 8, Article ID 085006, 2010.

[25] S. Miyazaki, T. Imai, Y. Igo, and K. Otsuka, "Effect of cyclic deformation on the pseudoelasticity characteristics of Ti-Ni alloys," *Metallurgical Transactions A*, vol. 17, no. 1, pp. 115–120, 1986.

[26] M. Dolce and D. Cardone, "Mechanical behaviour of shape memory alloys for seismic applications 2. Austenite NiTi wires subjected to tension," *International Journal of Mechanical Sciences*, vol. 43, no. 11, pp. 2657–2677, 2001.

[27] M. Kawaguchi, Y. Ohashi, and H. Tobushi, "Cyclic characteristics of pseudoelasticity of Ti-Ni alloys: effect of maximum strain, test temperature and shape memory processing temperature," *JSME International Journal. Ser. 1, Solid Mechanics, Strength of Materials*, vol. 34, no. 1, pp. 76–82, 1991.

[28] E. Choi, T. H. Nam, and Y. S. Chung, "Variation of mechanical properties of shape memory alloy bars in tension under cyclic loadings," *Materials Science and Engineering A—Structural Materials Properties Microstructure and Processing*, vol. 527, no. 16-17, pp. 4412–4417, 2010.

[29] M. I. Khan, H. Y. Kim, Y. Namigata, T.-H. Nam, and S. Miyazaki, "Combined effects of work hardening and precipitation strengthening on the cyclic stability of TiNiPdCu-based high-temperature shape memory alloys," *Acta Materialia*, vol. 61, no. 13, pp. 4797–4810, 2013.

[30] R. Delville, B. Malard, J. Pilch, P. Sittner, and D. Schryvers, "Transmission electron microscopy investigation of dislocation slip during superelastic cycling of Ni–Ti wires," *International Journal of Plasticity*, vol. 27, no. 2, pp. 282–297, 2011.

[31] R. Casati, F. Passaretti, and A. Tuissi, "Effect of electrical heating conditions on functional fatigue of thin NiTi wire for shape memory actuators," *Procedia Engineering*, vol. 10, pp. 3423–3428, 2011.

[32] J. Rejzner, C. Lexcellent, and B. Raniecki, "Pseudoelastic behaviour of shape memory alloy beams under pure bending: experiments and modelling," *International Journal of Mechanical Sciences*, vol. 44, no. 4, pp. 665–686, 2002.

[33] K. Wilde, P. Gardoni, and Y. Fujino, "Base isolation system with shape memory alloy device for elevated highway bridges," *Engineering Structures*, vol. 22, no. 3, pp. 222–229, 2000.

[34] E. Choi, D.-H. Lee, and N.-Y. Choei, "Shape memory alloy bending bars as seismic restrainers for bridges in seismic areas," *International Journal of Steel Structures*, vol. 9, no. 4, pp. 261–273, 2009.

[35] Y. Sutou, T. Omori, K. Yamauchi, N. Ono, R. Kainuma, and K. Ishida, "Effect of grain size and texture on pseudoelasticity in Cu-Al-Mn-based shape memory wire," *Acta Materialia*, vol. 53, no. 15, pp. 4121–4133, 2005.

[36] M. J. N. Priestley, F. Seible, and G. M. Calvi, *Seismic Design and Retrofit of Bridges*, John Wiley, New York, NY, USA, 1996.

[37] P. H. Leo, T. W. Shield, and O. P. Bruno, "Transient heat transfer effects on the pseudoelastic behavior of shape-memory wires," *Acta Metallurgica Et Materialia*, vol. 41, no. 8, pp. 2477–2485, 1993.